Extreme rainfall in Madeira: the June 2023 weather event

Tiago M. Ferreira[1,2] ,
Tomás H. Gaspar[1],
Maria O. Molina[1],
Ricardo M. Trigo[1],
Ricardo Deus[3] and
Alexandre M. Ramos[2]

[1] *Faculdade de Ciências, Instituto Dom Luiz, Universidade de Lisboa, Portugal*
[2] *Institute of Meteorology and Climate Research – Troposphere Research (IMKTRO), Karlsruhe Institute of Technology (KIT), Germany*
[3] *Divisão de Clima e Alterações Climáticas, Instituto Português do Mar e da Atmosfera, Lisbon, Portugal*

Introduction

An extreme precipitation event (EPE) occurred on Madeira Island between 5 and 6 June 2023, setting a new daily precipitation record for Portugal of 497.5mm (IPMA, 2023), surpassing the previous daily record of 333.8mm recorded in February 2010 (Fragoso *et al*., 2012). This maximum corresponds to the highest daily precipitation measurement recorded in the entire Portuguese network of meteorological stations since the beginning of systematic measurements more than 150 years ago. This event holds significance not only due to its daily record-breaking value, but also because it occurred in early summer; most of the EPEs over Madeira occur during the winter months (e.g. Fragoso *et al*., 2012; Couto *et al*., 2012).

 Madeira Island (the largest of the Archipelago of Madeira) spans an area of 740.7km² and is situated in the eastern subtropical region of the North Atlantic Ocean. The island's topography is marked by an east-to-west-oriented barrier, with the highest point reaching 1861m (Figure 1a). The island's orographic barrier stands nearly perpendicular to the prevailing southwesterly winds. Consequently, there is a notable contrast in temperature and precipitation between the northern (more humid) and southern slopes (Prada *et al*., 2009). The mean annual precipitation across the mountain varies considerably, ranging from approximately 600mm in the Funchal district (south part of the island) to nearly 3000mm at the summit of the eastern mountain range

(Prada, 2000; Prada *et al*., 2009; Baioni, 2011). There is a clear seasonal cycle in precipitation, with the highest values being recorded in the winter months, while the drier summer season only records an average monthly rainfall in the range of 2.9–6.6mm (Instituto de Meteorologia, 1999). The precipitation is often very intense, with a concentration that can reach values above 300mm in a single day, especially in autumn and early spring when very high-intensity rainfall occurs within a very short time (Baioni, 2011).

EPEs occurring over the western coast of the continental Iberian Peninsula (IP) during the winter months have been historically linked to major socio-economic impacts such as flooding, landslides, extensive property damage and human casualties. In continental IP, these EPEs are well documented (e.g. Liberato *et al*., 2012; Casanueva *et al*., 2014; Ramos *et al*., 2015, 2017); however, there have been considerably fewer studies on their occurrence over the Iberian Macaronesia Archipelagos (Azores, Madeira and Canary Islands), with exceptions related to catastrophic events (e.g. Andrade *et al*., 2008; Fragoso *et al*., 2012; Ramos *et al*., 2018; Díez *et al*., 2019). Flash floods constitute one of the most dangerous natural hazards in Madeira. Since 1800, at least 10 major events of disastrous flash floods have occurred, with the most recent outstanding event taking place on 20 February 2010, which caused 51 fatalities (Fragoso *et al*., 2012).

Several studies have made a comprehensive analysis of EPEs linked with atmospheric rivers (ARs) on Madeira Island (e.g. Couto *et al*., 2015; Ramos *et al*., 2018). ARs are long, narrow, and transient corridors of strong horizontal water vapour transport that are typically associated with a low-level jet ahead of the cold front of an extratropical cyclone (ETC; Ralph *et al*., 2018). The water vapour within these systems has its origin in tropical and/or extratropical sources (Gimeno *et al*., 2020; Pérez-Alarcón *et al*., 2022), the former being related to tropical moisture exports (Knippertz *et al*., 2013) and the latter related to the convergence of moisture along its path (Hu and Dominguez, 2019). In the last two decades, ARs have garnered interest as they are linked to a wide range of hydro-meteorological extremes, including the severity and frequency of floods and landslides, with large socio-economic impacts (Liberato *et al*., 2012; Trigo *et al*., 2016; Ferreira *et al*., 2025) and occasionally defining the end of a drought period (e.g.

Dettinger, 2013). In particular, extreme precipitation in Madeira was analysed between 1980 and 2010 for the extended winter months by Ramos *et al*. (2018), showing that 40% of the precipitation extremes occur in the presence of ARs in the region. In addition, Couto *et al*. (2015) analysed 10-year daily accumulated precipitation on Madeira and its relation to the meridional water vapour transport (occurring in ARs) between September 2002 and November 2012. Their findings show that ARs favour the occurrence of precipitation, although their presence is not the sole factor favouring high rainfall episodes in Madeira. Couto *et al*. (2015) suggest that the speed at which the moisture flux reaches the island, combined with the steep topography, may trigger certain physical processes that could intensify the precipitation occurrence. Fragoso *et al*. (2012) and Couto *et al*. (2012) concluded that the winter of 2010 was one of the wettest in Madeira, culminating in the AR-related event in February 2010, which was responsible for numerous landslides and flash flood events in the urban area of Funchal. In the case of June 2023, several impacts were recorded: at least 95 people were displaced from their homes (Hughes, 2023), the Madeira Airport experienced significant disruptions, and the Regional Civil Protection Service reported over 160 incidents (Gannon, 2023).

The EPE analysed in this study was associated with the occurrence of an ETC named *Oscar* (IPMA, 2023), centred at 36°N and 22°W in the early hours of 6 June 2023. This storm, and associated AR, resulted in substantial and prolonged precipitation, concurrent with intense wind gusts reaching 100kmh⁻¹ in the highlands and 80kmh⁻¹ in coastal regions (IPMA, 2023). This study aimed to unravel the synoptic conditions that led to the outstanding record-breaking extreme precipitation event over Madeira. The main objectives of this work are (1) to evaluate the spatial and temporal evolution of the precipitation associated with storm *Oscar*, and (2) to identify key elements of atmospheric circulation and the corresponding physical mechanisms that induced the record-breaking precipitation event observed on Madeira Island.

Data and methods

The large-scale data used in this study are the ECMWF (European Centre for Medium-Range Weather Forecasts) ERA5 reanalysis (Hersbach
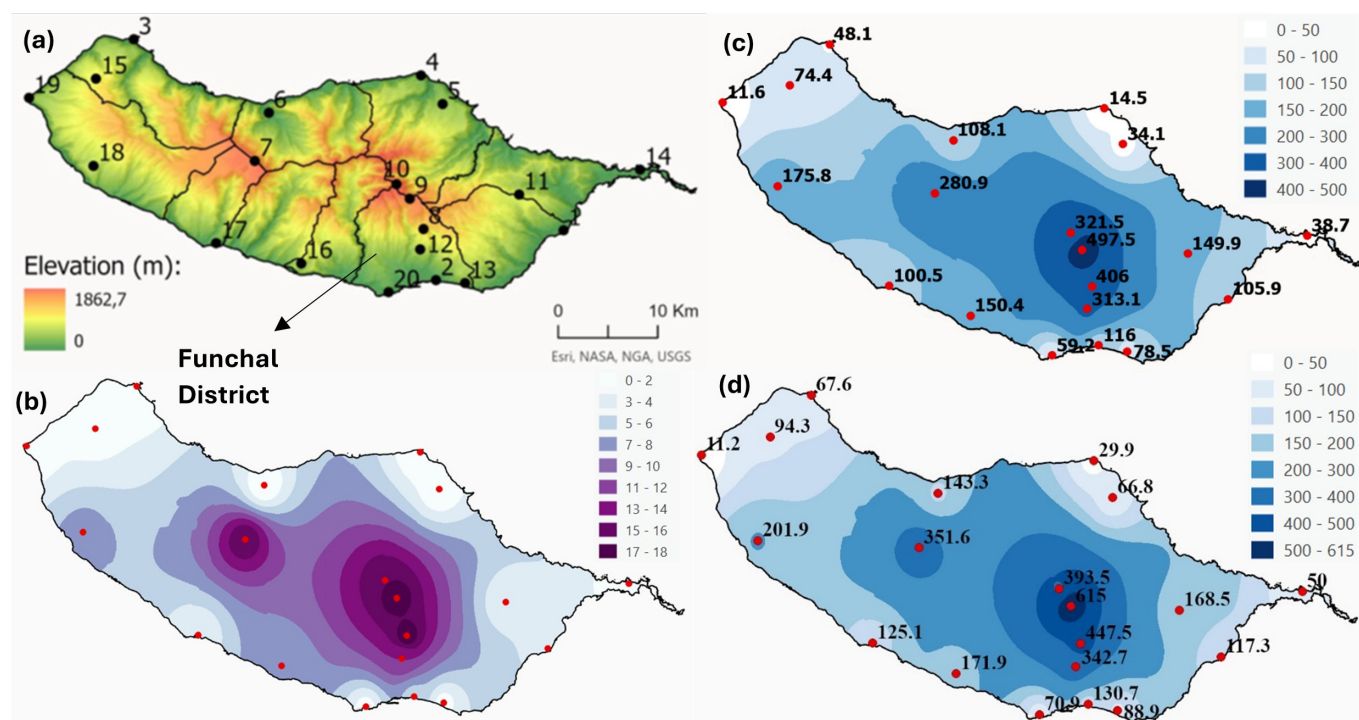
Figure 1. (a) Topography of the Madeira Island (Portugal) where black dots represent the locations of the rain gauge stations used in this study (names and description in Table A1). (b) Number of hours with precipitation above 10mm between 5 June, 0900 UTC and 6 June, 0900 UTC in 2023. (c) Total daily precipitation in Madeira from 5 June, 0900 UTC to 6 June, 0900 UTC in 2023. (d) Sliding 24h total accumulated precipitation from 5 June, 1400 UTC to 6 June 1400 UTC in 2023 (the 24h highest precipitation measurement). Red dots (on panels b, c, and d) represent the locations of the rain gauge stations used in this study (same points as a); names and description in Table A1.

et al., 2020). Several fields were extracted from both surface and specific atmospheric pressure levels. The former includes the mean sea-level pressure (SLP) and the sea surface temperature (SST). The latter include the zonal and meridional components of the vertically integrated water vapour transport (IVT, considering the entire atmospheric column); 200/850hPa divergence; 900hPa temperature; 250/850hPa wind; 850hPa specific humidity; and precipitation.

Data from 20 automated stations over the island were provided by the Portuguese Institute for Sea and Atmosphere (IPMA) with a 10min temporal resolution. To extend the assessment of this EPE to the entire island, we employ an inverse distance weighting approach (IDW – ArCGIS Pro n.d.). This method, also known as the inverse distance-based weighted interpolation, uses a weighted mean of nearby observations to estimate unknown values.

For the detection of AR events, we have implemented and adapted the global AR tracking method developed by Xu et al. (2020) and widely used in recent years (e.g. Fernández-Alvarez et al., 2023; Ferreira et al., 2025). The detection algorithm searches for ARs on an anomaly field that is calculated at each time step. In each IVT time step, the algorithm replaces each grid point with the minimum value that surrounds it; that is, it searches for the lowest value within the eight grid points around it.

This 'reconstructed' field is then subtracted from the original IVT, and the result (the anomaly) is used to detect AR objects. Afterwards, a threshold of $300\,kg\,m^{-1}\,s^{-1}$ is applied to the anomaly field, and to each region, the standard criteria for AR detection (length >2000km; width <1000km; length/width ratio >2) are implemented. More details on this method can be found in Xu et al. (2020). Additionally, in order to exclude tropical cyclone features from the analysis, we apply both a circularity criterion with a maximum value of 0.5 (following the work of Mahto et al., 2023) and a minimum value of 1000km to the distance between the first and last points of the AR axis.

Data on the inflow, outflow and ascent of moisture within the warm conveyor belt (WCB) were provided by KIT (Karlsruhe Institute of Technology). The method, developed by Quinting and Grams (2022), uses convolutional neural networks to obtain the footprints of the WCB inflow, ascent and outflow stages by obtaining conditional probabilities of WCB occurrences from predictors derived from temperature, geopotential height, specific humidity and horizontal wind components. The WCB air masses originate from the boundary layer in the warm sector of ETCs (WCB inflow, below 800hPa), ascend across the cyclones' warm front (WCB ascent, at least 600hPa ascent in 48h) and reach the upper troposphere (WCB outflow, above 400hPa).

The advanced detection methods employed in this study, while robust, are subject to specific uncertainties inherent to their algorithmic design. The AR method treats the IVT field as an image and applies techniques like thresholding, smoothing and connected-component labelling. While displaying lower sensitivity to parameters and a greater tolerance towards a wider range of water vapour flux intensities, the Gaussian smoothing applied to the IVT fields can alter the boundaries of ARs, either merging two nearby ARs or smoothing out a narrow AR. In addition, if an AR's strength decreases below the threshold, the algorithm might break a single long-lived AR into two separate tracks. Related to the WCB detection method, the most significant uncertainty is that the model provides a snapshot of WCB spatial footprints (based on conditional probabilities) but cannot discern the Lagrangian history of the identified air masses. This means that this method cannot directly quantify the ascent rate or source region of the WCB air; it is only possible to identify regions with a high probability of ongoing strong ascent. Despite these uncertainties, both methods (AR and WCB) represent significant advancements in objective feature detection. Their use allows for a consistent, reproducible and efficient analysis of a large number of events, which is well-suited for the purposes of this study.

Record-breaking extreme precipitation event

This section is focused on the assessment of the temporal and spatial distribution of the precipitation associated with this record-breaking EPE during 5 and 6 June 2023. The spatial pattern of accumulated precipitation in Madeira from 5 June, 0900 UTC to 6 June, 0900 UTC is presented in Figure 1c with the highest values obtained at the stations located at altitude, including the new daily record of 497.5 mm that was set for the Chão do Areeiro rain gauge station (station 9, Figure 1a). The names of the 20 meteorological weather stations are listed in Table A1. Historically, daily precipitation accumulation at IPMA stations is calculated between 0900 UTC of the previous day and 0900 UTC of the current day. However, when considering a 24h time frame, the highest value was measured from 5 June, 1400 UTC to 6 June, 1400 UTC in the high-altitude stations, reaching 615 mm at station Chão do Areeiro (Figure 1d). The spatial analysis reveals the presence of two predominant areas of exceptionally high precipitation, with accumulated values ranging from 300 to 500 mm. One area was situated across the mountain and southern slopes of the eastern mountain ranges, while the other was centrally positioned over the plateau sector. A closer look at Figure 1(d) indicates that the Funchal urban area (Station 2) was surrounded by extremely high values of precipitation associated with the south-eastern peak. Besides the total accumulated precipitation observed in several stations, this EPE is also characterised by a prolonged period of hours with significant precipitation values, shown in Figure 1(b) and showing the total number of hours with precipitation above 10 mm from 0900 on 5 June to 0900 UTC on 6 June. The duration of intense precipitation (>10 mmh⁻¹) was particularly long, ranging from 7 to 18 consecutive hours, namely over extensive areas situated in the highest regions of the island.

By analysing ERA5 precipitation data (Figure A1) on the same period as Figure 1c, we observe that although the extreme precipitation values are not visible in the reanalyses data, the highest values coincide with IPMA's *in situ* observations, located at the island's high-altitude stations. As we move towards the ocean, precipitation decreases; thus, we hypothesise that one of the factors responsible for this event was the topographic barrier of the island. While the ERA5 data is able to capture small-scale high-intensity values not captured in lower resolution reanalysis datasets due to the small area of the island, it is still unable to capture the observed values. Thus, while the highest values observed in the ERA5 reanalysis are between 70 and 80 mm, the *in situ* measurements present values above 400 mm on the top of the mountain.

In Table 1, a summary list of the most relevant metrics is presented, showcasing meteorological stations with the highest values of daily precipitation (0900–0900 UTC), as well as for the maximum measurement within 24h. Additionally, monthly values for June and the annual climatology are also presented, as well as past Junes' extremes and absolute extremes. Overall, results show that the absolute daily precipitation record for Madeira reached 497.5 mm, surpassing the previous absolute daily record of 333.8 mm obtained on 20 February 2010. Total precipitation for all represented stations significantly exceeded the climatological monthly values for June, even surpassing the previous June extreme event. Regarding the absolute extreme value at the daily scale, the June 2023 event only set a new daily record for the station Chão do Areeiro.

The effects of strong and continuous precipitation (Figure A2 – hourly maps between 5 June, 1400 UTC and 6 June, 0900 UTC) created critical conditions that in the past have triggered numerous landslides and other complex slope movements in these areas (Baioni, 2011; Fragoso *et al.*, 2012). However, on this occasion, such consequences did not occur, as this EPE was isolated, occurring at the beginning of the summer season following a sequence of dry spring months (DREM, 2023). Moreover, after the catastrophic event in February 2010, the Madeira government implemented several measures to make the island more resilient to flood damage (Cordero, 2010). The range of these measures included regulation of the water courses, construction of huge solid slit dams for sediment management, redesigning and rebuilding drainage channels and development of an early warning system (Cordero, 2010; Caires *et al.*, 2020).

Large-scale atmospheric conditions

The synoptic evolution of the storm *Oscar* (IPMA, 2023) and the key elements of large-scale atmospheric circulation largely responsible for the record-breaking precipitation event are now analysed. The synoptic evaluation using the IVT, AR characteristics, SLP and WCB data are shown in Figure 2 for Days 5 and 6, at 0000 and 1200 UTC. By 5 June 0000 UTC (Figures 2a and b), two relatively weak low-pressure systems were present over the western and eastern sectors of the North Atlantic Ocean, respectively. Both systems are connected by a very strong zonal AR that covers most of the north Atlantic basin. The air masses along the AR are characterised by very humid and hot air (potential temperature above 320K, Figure A3) and are positioned south of the cold front (Figure A4 – weather charts from the German Weather Service, DWD, available at https://www.wetter3.de/). Focusing now only on the eastern North Atlantic Ocean storm, in the subsequent hours (Figures 2c and d), there was a deepening of the low-pressure system *Oscar*, presenting multiple centres while moving eastwards. In addition, the maximum IVT values inside the AR increased, from 1327 to 1518 kgm⁻¹s⁻¹, occurring close to the centre of the low-pressure centre. By 6 June 0000 UTC (Figures 2e and f), the central pressure of the eastern cyclone had decreased to

---

Table 1

Summary of meteorological stations with highest daily precipitation values registered during the 5/6 June 2023 event. June and annual climatological (1971–2000) values are presented, along with the former June extremes and absolute extremes. Both records of this event are presented in bold.

| Station	Daily max. (mm)	24h max. (mm)	Climatological June (71-00)	Climatological annual (71-00)	Previous June extreme (mm)	Previous June extreme Date (day-year)	Extreme absolute (mm)	Extreme absolute Date	Since Date
Santana	34.1	69.4	44.5	1399.6	134.0	06/1966	217.0	06/03/2001	01/01/1942
Bica da Cana	280.9	354.0	66.0.	2635.4	212.0	21/1964	327.2	26/01/2011	01/01/1961
Chão do Areeiro	**497.5**	**615.0**	48.2	2620.0	282.3	01/1965	**497.5**	06/06/2023	01/01/1961
Lugar de Baixo	100.5	131.1	8.9	600.2	68.8	21/1964	111.9	26/11/2010	01/01/1961
Santa Catarina Aeroporto	105.9	121.0	9.0	693.6	67.9	06/2020	147.4	21/02/2010	01/01/1961
Funchal Obs.	116.0	134.0	6.4	596.4	57.8	21/1964	292.7	28/03/2021	01/01/1949
Porto Santo	36.3	6.0	7.0	361.3	32.4	13/2006	90.0	26/01/2011	01/01/1961

![RMetS Royal Meteorological Society]
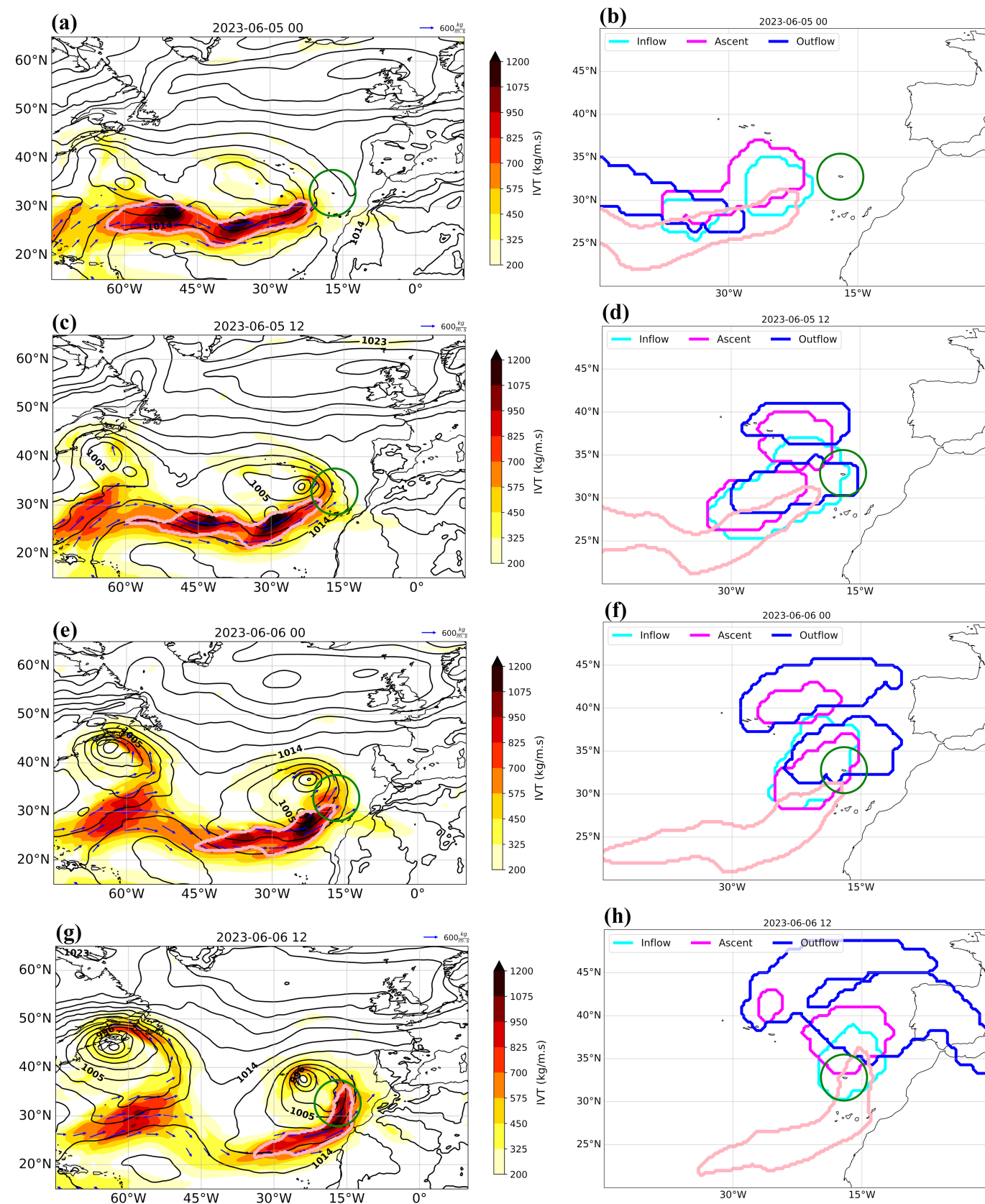
Figure 2. (Left column) Spatial pattern of vertically integrated water vapour transport (IVT, shaded) and IVT vectors (blue contours), for 5 June, 0000 UTC (a) and 1200 UTC (c) and for 6 June, 0000 UTC (e) and 1200 UTC (g). The SLP contour lines are represented in black. The bolder light-pink contour around the highest values of IVT represents the AR spatial configuration. (Right column) Warm Conveyor Belt data, with the bolder contour lines representing inflow (light-blue contour), ascent (pink contour) and outflow (blue contour), for 5 June, 0000 UTC (b) and 1200 UTC (d) and for 6 June, 0000 UTC (f) and 1200 UTC (h). The light-pink contour represents the AR spatial configuration. The green circle (on both columns) represents the Madeira Island's region, with the center corresponding to the location of the island.

996hPa, and the cold front approached the warm front, leading to a gradual narrowing of the warm sector (shown in Figure A4). At this time step, Madeira Island is still outside the detected AR but intense IVT values are visible near the region, justifying the persis- tent precipitation that occurred since 5 June at 1300 UTC (Figure A2). On 6 June 1200 UTC (Figures 2g and h), the central pressure fur-

RMetS
Royal Meteorological Society

ther dropped to 991hPa, becoming stationary west of the Madeira Islands for approximately 36h, carrying within its circulation a mass of warm, unstable air with a high water vapour content. The WCB region (Figure 2 right column) shows that Madeira Island was embedded within a region of both inflow and ascent of moisture. This strong, organised ascent within the WCB is a key driver for upper level divergence, as mass is transported vertically and then spreads out anticyclonically in the upper troposphere. This divergence aloft, in turn, promotes lower surface pressure and intensification of the cyclonic circulation at the surface (as seen on *Oscar's* SLP data), having its maximum intensity of 995hPa on Day 6, 1200 UTC (value stated by IPMA; observed on Figure 2g with a value of 996hPa). Thus, the presence of the WCB not only provided the moisture reservoir and vertical uplift necessary for the extreme precipitation but also contributed to the dynamical forcing that maintained the storm itself.

In order to analyse the possible dynamic lifting, we show the horizontal wind divergence at two different levels (250 and 850hPa) with the results being shown in
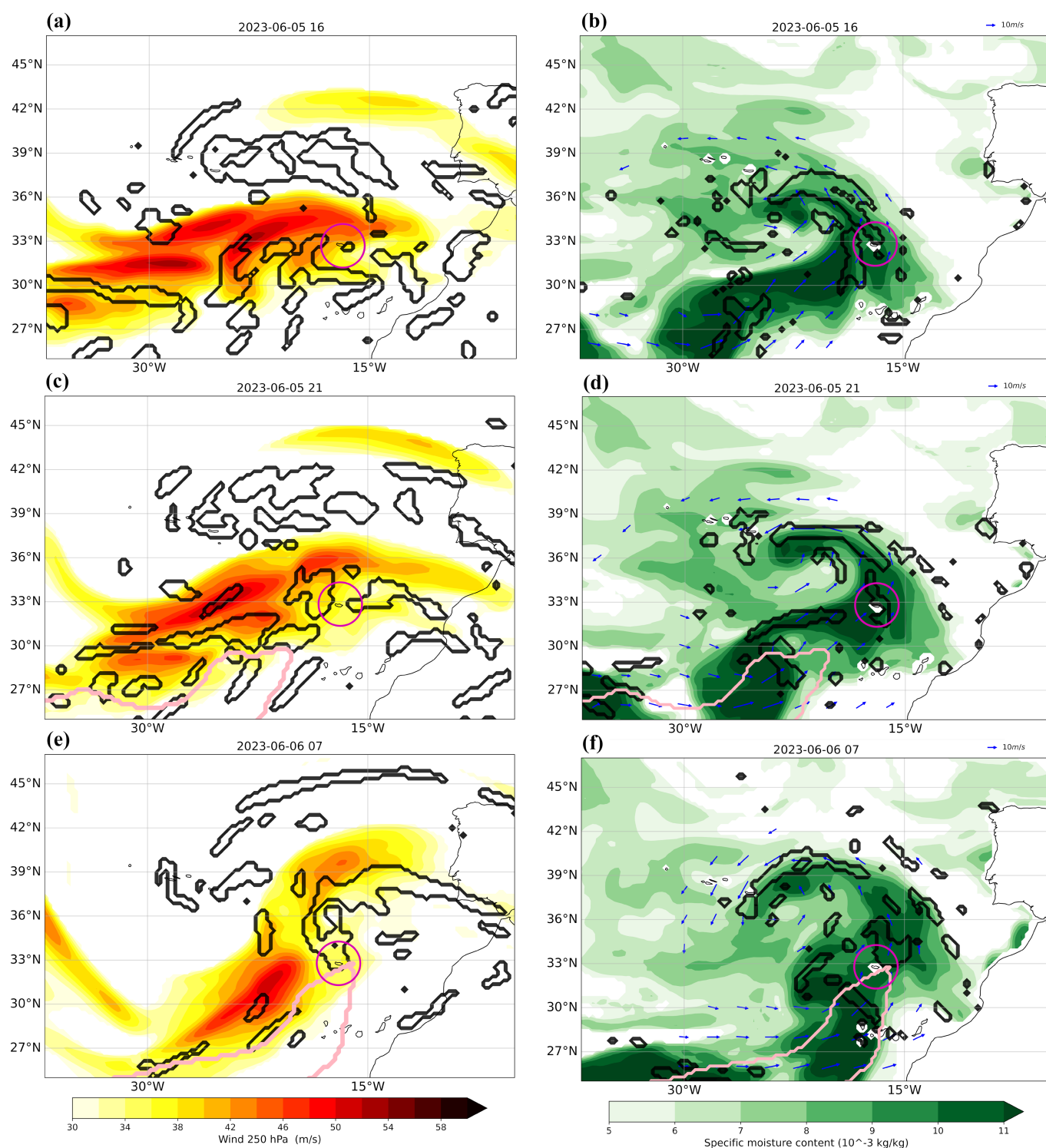

Figure 3. (Left column) Wind speed (colours, units in ms^{-1}) and divergence at 250hPa pressure level (contour lines, values higher than $0.3 \times 10^{-4}s^{-1}$), for 5 June 2023, 1600 UTC (a) and 2100 UTC (c) and for 6 June, 0700 UTC (e). Light-pink contour line represents the AR area (once detected) and thin green line inside represents its axis. (Right column) Wind speed (arrows, units in ms^{-1}), specific moisture content (colours, units in $10^{-3}kgkg^{-1}$), wind convergence (contour lines, values lower than $-0.3 \times 10^{-4}s^{-1}$) at the 850hPa pressure level, for 5 June 2023, 1600 UTC (b) and 2100 UTC (d) and for 6 June, 0700 UTC (f). Light-pink contour line represents the AR area (once detected). The pink circle represents the Madeira Island's region, with the center corresponding to the location of the island.

Figure 3, where positive values correspond to divergence and negative values to convergence. The upper level wind speed (at 250hPa) and associated wind divergence (as shown as values $0.3 \times 10^{-3} s^{-1}$) are analysed specifically for the critical periods of intense precipitation on 5 and 6 June (Figure 3 left panels). The peak precipitation hour on 5 June was identified as occurring between 1500 and 1600 UTC (Figure A2). Results show that, during this period, the upper air jet stream (the subtropical jet stream) was positioned over the Eastern Atlantic, spanning latitudes between 30 and 35 N (Figure 3a). By 2100 UTC, the Madeira region was located exactly beneath the northward jet exit zone, a region known for generating upper level divergence due to the deceleration of the wind flow. This divergence is evident in the contours directly over and near the island (Figure 3c), which is a classic signature of large-scale upward motion according to the quasi-geostrophic theory (mass conservation requires ascent below a region of upper-level divergence to compensate for the horizontal spreading of air). This observation supports the hypothesis that large-scale forcing played a pivotal role in triggering the high precipitation that impacted Madeira between 2100 and 2200 UTC (Figure A2). In the subsequent hours, the region with the most pronounced upper air divergence shifted southwesterly; however, Madeira continued to experience favourable large-scale conditions conducive to substantial vertical movements (Figure 3e).

Finally, the lower 850hPa wind speed fields and wind convergence (where values of divergence below $-0.3 \times 10^{-3} s^{-1}$) are also analysed in Figure 3 (right panels). These two low tropospheric fields are useful to show if conditions for deep convection were present during the event. They reveal strong low-level southwesterlies, reaching wind speeds of up to 20ms^{-1} over the region during the three time steps that

were analysed. Notably, this pressure level corresponds roughly to the elevated terrain of the island (Fragoso *et al.*, 2012). This circulation pattern, associated with the presence of the AR, increased the advection of high values of humidity with a southwest–northeast orientation (Figure 3, AR area), located within the warm sector of the cyclone (Figure A4). Consequently, this notable surplus of humidity, within the AR and illustrated by the specific humidity at the 850hPa geopotential level, reached the Madeira region when other favourable dynamic mechanisms for deep convection were already in progress, including upper level divergence and frontal uplift. Figure 3 right panels also depict low-level convergence, a robust indicator for large-scale precipitation, suggesting that Madeira experienced conducive large-scale conditions between the afternoon of 5 June and the early morning of 6 June.

Above, we have shown that the various dynamic elements converged close to Madeira, where the complex orography characterised by an E-W-oriented mountain range might have acted as an amplifying factor for generating precipitation. Thus, we are confident that the occurrence of an extreme AR (with the maximum IVT higher than 1000kgm^{-1}s^{-1} for more than 24h), responsible for large southwesterly moisture flux transport, combined with upper air divergence, the relative position of the jet stream, and the availability of a very humid and hot air mass over the Madeira region were key elements to account for the occurrence of this strong event that struck Madeira.

Finally, positive SST anomalies (in reference to the 1980 to 2022 climatology) above 1°C occurred during the 2 weeks prior to the event, across a wide region (Figure 4). These abnormally high SSTs, often led to an increase in the evaporation rates that consequentially increase the atmospheric water vapour content and also induce baroclinic
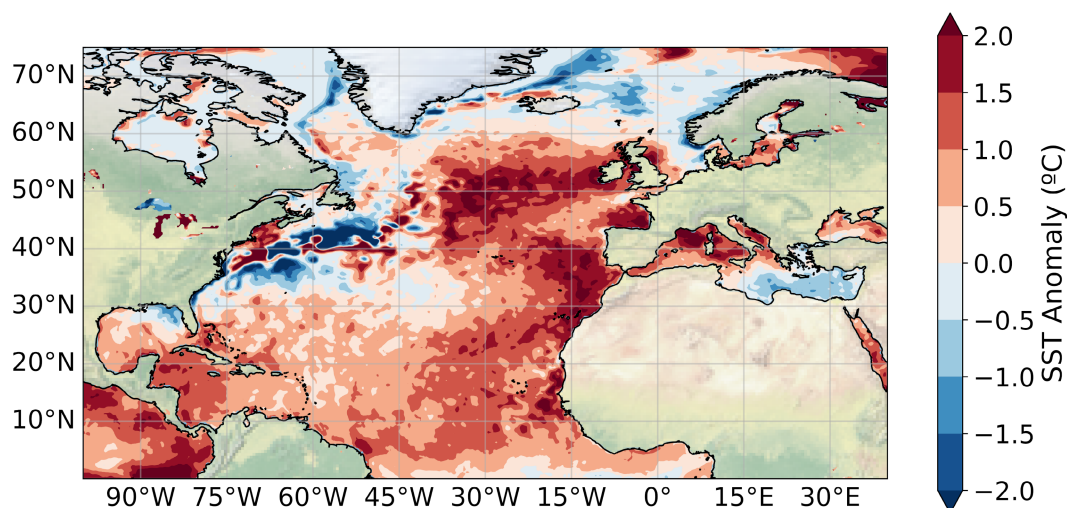
instabilities in the overlying atmosphere (Tompkins, 2001; Ye and Tozuka, 2022), that lead to the formation of both ETCs and ARs (e.g. Trenberth and Fasullo, 2007).

Conclusions

In the early summer of 2023, Madeira Island (Portugal) was struck by a complex ETC, named *Oscar*, and an associated AR on 5/6 June 2023. This event led to a new daily precipitation record, with 497.5mm measured at the highest peak of Madeira Island (Station 9, Chão do Areeiro, 1590m). Besides becoming the new daily record for the island (surpassing the previous 333.8mm in February 2010), this value is also the highest measurement in the entire Portuguese territory since the mid-nineteenth century. Notably, this event occurred just 13 years after the 2010 record, much sooner than the 90-year return period estimated by Fragoso *et al.* (2012).

This study aimed to characterise the exceptionally heavy rainfall during the June 2023 Extreme Precipitation Event (EPE) on Madeira Island from two different perspectives: the first focuses on the spatial and temporal distribution of precipitation across the island and the associated records, and the second on the assessment of the synoptic situation that led to the event.

In relation to our first research objective, the results show that the spatial extent of precipitation was significant, with more than 50% of the island recording total precipitation values exceeding 200mm (accumulated between 0900 UTC of Day 5 and 0900 UTC of Day 6). Two main areas exhibited precipitation accumulations ranging between 300 and 615mm: one located over the uplands and southern slopes of the eastern mountains, and the other centred over the central plateau. Additionally, in the mountainous regions, precipitation greater than 10mm per hour was recorded for more than nine consecutive hours.

Figure 4. SST mean anomaly from 29 May to 5 June 2023 (29 May, 0000 UTC to 4 June, 1800 UTC), with reference to the 1980–2022 period.

RMetS
Royal Meteorological Society

Regarding the mechanisms associated with this event – our second research question – the results show that strong upper level divergence, combined with intense low-level convergence and the unusually low-latitude position of the jet stream, created favourable conditions for the uplift of moisture from the AR, leading to significant precipitation. Furthermore, the WCB of the ETC exhibited a clear convective circulation directly over Madeira Island, characterised by strong inflow and vertical moisture transport, which also contributed to the exceptionally high precipitation totals.

In recent years, there has been a growing number of studies highlighting the importance of ARs not only for freshwater resources but also as key drivers of extreme precipitation events with significant socio-economic impacts (Dettinger *et al*., 2011; Lavers and Villarini, 2013; Ralph *et al*., 2019). Substantial efforts have been made to analyse the relationship between ARs and large-scale atmospheric circulation. In this study, we show that the presence of the AR, along with the inflow and ascent within the WCB, acted both as a moisture source and an uplift mechanism, contributing to the occurrence of the extreme event. While the connection between WCBs and fronts (e.g. Catto *et al*., 2015), as well as between fronts alone (e.g. Catto *et al*., 2012; Catto and Pfahl, 2013) and EPEs has been previously established, the link between ARs and such events has so far only been explored from a climatological perspective (e.g. Sodemann *et al*., 2020).

This study highlights the importance of the connection between the WCB and the AR in the occurrence of the extreme precipitation event, by illustrating a possible link between the moisture advection within the AR and the convective motion associated with the ascent phase of the WCB. An AR is identified as a filamentary region of enhanced IVT, effectively marking the plume of moisture. In contrast, a WCB is defined by the strong ascent of air parcels within a cyclone, representing a key dynamical process that forces this moisture to ascend, cool, and precipitate. While these features are physically linked and often overlap – as WCBs are frequently the mechanism responsible for the intense precipitation within ARs – they are diagnosed using different criteria and highlight different aspects of the system. The spatial configuration observed in this case, with the WCB ascent region located at the poleward-leading edge of the AR, is a common feature of mature cyclones. Analysing both allows us to not only quantify the available moisture (via the AR) but also to directly diagnose the triggering mechanism for the EPE (via the WCB). The interaction between ARs and large-scale atmospheric circulation features, such as ETCs, WCBs and frontal systems– has

been extensively studied in recent decades, with the aim of improving the prediction of these systems and the associated EPEs (Lavers *et al*., 2020a,b; DeHaan *et al*., 2023). Moreover, this study contributes to the broader context of ongoing climate change, where rising global mean surface temperatures have increased the atmosphere's water-holding capacity (as described by the Clausius–Clapeyron relationship), thereby enhancing both the likelihood and intensity of both the AR development/intensity and the occurrence of extreme precipitation events (IPCC, 2021).

Acknowledgements

Author contributions

Tiago M. Ferreira: Conceptualization; methodology; investigation; formal analysis; writing – original draft; writing – review and editing; visualization. **Tomás H. Gaspar:** Conceptualization; methodology; writing – original draft; investigation; visualization. **Maria O. Molina:** Writing – original draft; writing – review and editing; methodology. **Ricardo M. Trigo:** Conceptualization; methodology; investigation; funding acquisition; supervision; writing – original draft; writing – review and editing. **Ricardo Deus:** Writing – original draft; writing – review and editing; data curation. **Alexandre M. Ramos:** Conceptualization; investigation; funding acquisition; writing – review and editing; methodology; supervision.

Conflict of interest statement

All authors declare that they have no conflicts of interest.

Data availability statement

ERA5 reanalyses are available from the Copernicus Climate Data Store (https://doi.org/10.24381/CDS.ADBB2D47, Copernicus Climate Change Service, 2023). The DWD surface maps are freely available through the following archive (https://wetter3.de/

archiv_dwd_dt.html). The WCB data were accessed through the LSDF Online Storage service of KIT, provided by Quinting and Grams (2022).

Supporting Information

Additional supporting information may be found online in the Supporting Information section at the end of the article.
Table A1.

References

Andrade C, **Trigo RM**, **Freitas MC** *et al*. 2008. Comparing historic records of storm frequency and the North Atlantic Oscillation (NAO) chronology for the Azores region. *Holocene* **18**(5): 745–754. https://doi.org/10.1177/0959683608091794

Baioni D. 2011. Human activity and damaging landslides and floods on Madeira Island. *Nat. Hazards Earth Syst. Sci.* **11**: 3035–3046. https://doi.org/10.5194/nhess-11-3035-2011

Caires M, **Miranda T**, **Santos TP** *et al*. 2020. O dia que mudou a Madeira para sempre [grande reportagem], Expresso. https://expresso.pt/arquivo/multimedia-expresso/2020-02-19-O-dia-que-mudou-a-Madeira-para-sempre-grande-reportagem (accessed 28 May 2025).

Casanueva A, **Rodríguez-Puebla C**, **Frías MD** *et al*. 2014. Variability of extreme precipitation over Europe and its relationships with teleconnection patterns. *Hydrol. Earth Syst. Sci.* **18**: 709–725. https://doi.org/10.5194/hess-18-709-2014

Catto JL, **Jakob C**, **Berry G** *et al*. 2012. Relating global precipitation to atmospheric fronts. *Geophys. Res. Lett.* **39**: L10805. https://doi.org/10.1029/2012GL051736

Catto JL, **Madonna E**, **Joos H** *et al*. 2015. Global relationship between fronts and warm conveyor belts and the impact on extreme precipitation. *J. Clim.* **28**: 8411–8429. https://doi.org/10.1175/JCLI-D-15-0171.1

Catto JL, **Pfahl S**. 2013. The importance of fronts for extreme precipitation. *J. Geophys. Res. Atmos.* **118**: 10,791–10,801. https://doi.org/10.1002/jgrd.50852

Cordero M. 2010. Portugal: EIB loan for Madeira Flood Damage Reconstruction, European Investment Bank. https://www.eib.org/en/press/all/2010-203-portugal-eib-loan-for-madeira-flood-damage-reconstruction (accessed 28 May 2025).

Couto FT, **Salgado R**, **Costa MJ**. 2012. Analysis of intense rainfall events on Madeira Island during the 2009–2010 winter. *Nat. Hazards Earth Syst. Sci.* **12**: 2225–2240. https://doi.org/10.5194/nhess-12-2225-2012

Couto FT, **Salgado R**, **Costa MJ**, **Prior V**. 2015. Precipitation in the Madeira Island over a 10-year period and the meridional water vapour transport during the winter seasons. *Int. J. Climatol.* **35**: 3748–3759. https://doi.org/10.1002/joc.4243

DeHaan LL, **Wilson AM**, **Kawzenuk B** *et al*. 2023. Impacts of dropsonde observations on forecasts of atmospheric rivers

and associated precipitation in the NCEP GFS and ECMWF IFS models. *Weather Forecast.* **38**: 2397–2413. https://doi.org/10.1175/WAF-D-23-0025.1

Dettinger MD. 2013. Atmospheric rivers as drought busters on the U.S. West Coast. *J. Hydrometeorol.* **14**(6): 1721–1732. https://doi.org/10.1175/JHM-D-13-02.1

Dettinger MD, Ralph FM, Das T *et al*. 2011. Atmospheric rivers, floods and the water resources of California. *Water* **3**: 445–478. https://doi.org/10.3390/w3020445

Díez AL, Suárez PM, Pacheco JD *et al*. 2019. Rainfall and flooding in coastal tourist areas of the Canary Islands (Spain). *Atmos.* **10**(12): 809. https://doi.org/10.3390/atmos10120809

DREM – **Direção Regional de Estatistica da Madeira**: Precipitation (monthly) – 2012-2023. 2023 https://estatistica.madeira.gov.pt/en/download-now-3/territorio-gb/weather-data/weather-data-time-series/category/674-weather-data-time-series.html (accessed 28 May 2025)

Ferreira TM, Trigo RM, Gaspar TH *et al*. 2025. The record-breaking precipitation event of December 2022 in Portugal. *Nat. Hazards Earth Syst. Sci.* **25**: 609–623. https://doi.org/10.5194/nhess-25-609-2025

Fernández-Alvarez JC, Pérez-Alarcón A, Eiras-Barca J *et al*. 2023. Changes in moisture sources of atmospheric rivers landfalling the Iberian Peninsula with WRF-FLEXPART. *J. Geophys. Res. Atmos.* **128**: e2022JD037612. https://doi.org/10.1029/2022JD037612

Fragoso M, Trigo RM, Pinto JG *et al*. 2012. The 20 February 2010 Madeira flash-floods: synoptic analysis and extreme rainfall assessment. *Nat. Hazards Earth Syst. Sci.* **12**: 715–730. https://doi.org/10.5194/nhess-12-715-2012

Gannon, S. 2023. New historic rainfall maximum recorded. *Madeira Weekly*. https://madeira-weekly.com/2023/06/10/new-historic-rainfall-maximum-recorded/ (accessed: 28 May 2025)

Gimeno L, Vazquez M, Eiras-Barca J *et al*. 2020. Recent progress on the sources of continental precipitation as revealed by moisture transport analysis. *Earth Sci. Rev.* **201**: 103070. https://doi.org/10.1016/j.earscirev.2019.103070

Hersbach H, Bell B, Berrisford P *et al*. 2020. The ERA5 global reanalysis. *Q. J. R. Meteorol. Soc.* **146**: 1999–2049. https://doi.org/10.1002/qj.3803

Hu H, Dominguez F. 2019. Understanding the role of tropical moisture in atmospheric rivers. *J. Geophys. Res. Atmos.* **124**: 13826–13842. https://doi.org/10.1029/2019JD030867

Hughes, T. 2023. Madeira resists record rain. *Madeira Island News*. https://www.madeiraislandnews.com/2023/06/madeira-resists-record-rain.html (accessed 28 May 2025).

IDW (Spatial Analyst) – **ArCGIS Pro | Documentation**. n.d. https://pro.arcgis.com/en/pro-app/latest/tool-reference/spatial-analyst/idw.htm#L_

Instituto de Meteorologia, I. P. 1999. Climate data – Funchal/Madeira [Report]. Ministério da Ciência, Tecnologia e Ensino Superior https://www.ipma.pt/bin/file.data/climate-normal/cn_71-00_FUNCHAL.pdf (accessed 28 May 2025).

IPCC: Climate Change 2021. 2021. The physical science basis, in Contribution of Working Group I to the Sixth Assessment Report of the Intergovernmental Panel on Climate Change. Masson-Delmotte V, Zhai P, Pirani A *et al*. (eds). Cambridge University Press: Cambridge, UK and New York, NY. https://doi.org/10.1017/9781009157896.

IPMA. Precipitação Histórica na Madeira – 5 e 6 de junho de 2023. Instituto português do mar e da atmosfera (ipma) climate report, 2023. 2023 https://www.ipma.pt/pt/media/noticias/documentos/2023/Noticia_Precipitacao_Madeira_pt3_vrs_FES_4_RD_09062023.pdf (accessed 8 October 2023).

Knippertz P, Wernli H, Gläser G. 2013. A global climatology of tropical moisture exports. *J. Clim.* **26**(10): 3031–3045. https://doi.org/10.1175/JCLI-D-12-00401.1

Lavers DA, Ingleby NB, Subramanian AC *et al*. 2020a. Forecast errors and uncertainties in atmospheric rivers. *Weather Forecast.* **35**: 1447–1458. https://doi.org/10.1175/WAF-D-20-0049.1

Lavers DA, Ralph FM, Richardson DS *et al*. 2020b. Improved forecasts of atmospheric rivers through systematic reconnaissance, better modelling, and insights on conversion of rain to flooding. *Commun. Earth Environ.* **1**: 39. https://doi.org/10.1038/s43247-020-00042-1

Lavers DA, Villarini G. 2013. The nexus between atmospheric rivers and extreme precipitation across Europe. *Geophys. Res. Lett.* **40**: 3259–3264. https://doi.org/10.1002/grl.50636

Liberato MLR, Ramos AM, Trigo RM *et al*. 2012. Moisture sources and large-scale dynamics associated with a flash flood event. *Geoph. Monog. series* **200**: 111–126. https://doi.org/10.1029/2012GM001244

Mahto SS, Nayak MA, Lettenmaier DP *et al*. 2023. Atmospheric rivers that make landfall in India are associated with flooding. *Commun. Earth Environ.* **4**: 120. https://doi.org/10.1038/s43247-023-00775-9

Pérez-Alarcón A, Sorí R, Fernández-Alvarez JC *et al*. 2022. Where does the moisture for North Atlantic tropical cyclones come from? *J. Hydrometeorol.* **23**: 457–472. https://doi.org/10.1175/JHM-D-21-0117.1

Prada SLRN. 2000. Geologia e recursos hidricos subterraneos da Ilha da Madeira Tese de Doutoramento. Universidade da Madeira. Universidade da Madeira – Unidade de Documentação e Arquivo. http://hdl.handle.net/10400.13/118 (accessed 28 May 2025).

Prada S, Sequeira MM, Figueira C *et al*. 2009. Fog precipitation and rainfall interception in the natural forests of Madeira Island (Portugal). *Agric. For. Meteorol.* **149**(6–7): 1179–1187, ISSN 0168-1923. https://doi.org/10.1016/j.agrformet.2009.02.010

Quinting JF, Grams CM. 2022. EuLerian identification of ascending AirStreams (ELIAS 2.0) in numerical weather prediction and climate models – Part 1: Development of deep learning model. *Geosci. Model Dev.* **15**(2): 715–730. https://doi.org/10.5194/gmd-15-715-2022

Ralph FM, Dettinger MCLD, Cairns MM *et al*. 2018. Defining "Atmospheric river": how the glossary of meteorology helped resolve a debate. *Bull. Am. Meteor. Soc.* **99**(4): 837–839. https://doi.org/10.1175/BAMS-D-17-0157.1

Ralph FM, Rutz JJ, Cordeira JM *et al*. 2019. A scale to characterize the strength and impacts of atmospheric rivers. *Bull. Amer. Meteor. Soc.* **100**: 269–289. https://doi.org/10.1175/BAMS-D-18-0023.1

Ramos AM, Trigo RM, Liberato MLR. 2017. Ranking of multi-day extreme precipitation events over the Iberian Peninsula. *Int. J. Climatol.* **37**: 607–620. https://doi.org/10.1002/joc.4726

Ramos AM, Trigo RM, Liberato MLR *et al*. 2015. Daily precipitation extreme events in the iberian peninsula and its association with atmospheric rivers. *J. Hydrometeorol.* **16**: 579–597. https://doi.org/10.1175/JHM-D-14-0103.1

Ramos AM, Trigo RM, Tomé R *et al*. 2018. Impacts of atmospheric rivers in extreme precipitation on the European Macaronesian Islands. *Atmosphere* **9**(8): 325. https://doi.org/10.3390/atmos9080325

Sodemann H, Wernli H, Knippertz P *et al*. 2020. Structure, process and mechanism, in Atmospheric Rivers. Springer, pp 284. https://doi.org/10.1007/978-3-030-28906-5_2.

Tompkins AM. 2001. On the relationship between tropical convection and sea surface temperature. *J. Clim.* **14**: 633–637. https://doi.org/10.1175/1520-0442(2001)014<0633:OTRBTC>2.0.CO;2

Trenberth KE, Fasullo J. 2007. Water and energy budgets of hurricanes and implications for climate change. *J. Geophys. Res.* **112**: D23107. https://doi.org/10.1029/2006JD008304

Trigo RM, Ramos C, Pereira SS *et al*. 2016. The deadliest storm of the 20th century striking Portugal: flood impacts and atmospheric circulation. *J. Hydrol.* **541**(Part A): 597–610. https://doi.org/10.1016/j.jhydrol.2015.10.036

Xu G, Ma X, Chang P *et al*. 2020. Image-processing-based atmospheric river tracking method version 1 (IPART-1). *Geosci. Model Dev.* **13**(10): 4639–4662. https://doi.org/10.5194/gmd-13-4639-2020

Ye Z, Tozuka T. 2022. Causal relationship between sea surface temperature and precipitation revealed by information flow. *Front. Clim.* **4**: 1024384. https://doi.org/10.3389/fclim.2022.1024384

Correspondence to: A. M. Ramos
alexandre.ramos@kit.edu

RMetS
Royal Meteorological Society